



# Ground Reaction Force Estimation of a Prosthetic Leg Using Optimized Derivative-Free Kalman Filter

Y. M. Zakari, T. H. Sikiru\*, Y. A. Sha'aban, C. M. Ogbonna

Department of Computer Engineering, Ahmadu Bello University, Zaria, Nigeria

\*[thsikiru@abu.edu.ng](mailto:thsikiru@abu.edu.ng)

Research Article

## Abstract

Artificial Prosthesis Systems assists injured patients to improve their quality of life. For proper utilization of these artificial systems, accurate estimation of external forces and state vectors are required for feedback control. Existing works estimate ground reaction forces using load cells and extended Kalman filter. However, load cells are expensive, bulky and prone to errors, whereas the filter has some inherent limitations which occur as a result of the truncation of higher order terms brought about by local linearization using first-order Taylor-series approximation and also requires Jacobian computation. We propose a robust Kalman filtering approach known as an optimized derivative-free Kalman filter for the estimation of states and ground reaction forces of a prosthesis system for transfemoral (TF) amputees. The system has four degrees of freedom (vertical displacement, thigh angle, knee angle and ankle angle). The plant is transformed to its linear equivalent using differential flatness. Grasshopper optimization algorithm was employed to optimize the parameters of the derivative-free Kalman filter by minimizing the root mean square estimation error of the nonlinear filter. Four measurement sensors were used (vertical displacement, thigh angle, knee angle and ankle angle) and the performance of the prosthesis system in normal gait mode was examined. The designed filter was simulated on Matlab R2018a and the results are compared with extended Kalman filter and unscented Kalman filter. The superiority of our method in estimating the joint angle reference, the GRFs and the reduction of material cost are shown when compared with existing methods. The optimized derivative-free Kalman filter recorded an average RMSE improvement of 99.85% and 99.77% estimation in joint angles and GRFs when computed and compared to existing methods.

Copyright © Faculty of Engineering, Ahmadu Bello University, Zaria, Nigeria.

## Keywords

Derivative-free Kalman filter; grasshopper optimization; ground reaction force; prosthetic; transfemoral amputees.

## Article History

Received: June, 2022

Reviewed: July, 2022

Accepted: August, 2022

Published: August, 2022

## 1. Introduction

Advances in technology continues to improve the quality of life of patients in various forms and degrees. Artificial prosthetic systems continue to make themselves relevant in the life of patients that have suffered injuries as they significantly ease the effects on patients that have suffered amputation. The main aim of every prosthetic leg is to provide a gait similar to that of a normal person. To achieve this aim, accurate estimation of the system states and ground reaction forces (GRFs) are needed for feedback control (Fakoorian *et al.*, 2017). From being used mainly as cosmetic purposes in ancient Egyptians to rehabilitation purposes in prosthetic, transfemoral amputees, derivative-free Kalman filter, state estimation, grasshopper optimization, ground reaction force Roman civilization, prosthesis systems have gained considerable attention in recent times where advances in microelectronics and robotic technologies have become the order of the day (Moosavi *et al.*, 2017). From passive prosthesis systems, semi-active artificial limb prosthesis have been developed (Awad *et al.*, 2016; Zhang *et al.*, 2021). Nowadays, researchers' attention has been turned to active prosthetic systems (Varol and Goldfarb, 2007; Geng *et al.*, 2010; Geng *et al.*, 2012; Behera and Indalkar, 2020). The

main difference between active and semi-active prosthetic systems is that the former has an inherent capability of autonomous generation of forces (Varol and Goldfarb, 2007; Windrich *et al.*, 2016). Indeed, considerable efforts have been made by researchers in order to rehabilitate walking in patients who have suffered from amputation as recently reviewed by Windrich *et al.* (2016).

The robots/prosthetics leg model are non-linear systems (Ron Davis, 2014), hence they are usually linearized before appropriate estimation method and control measures are applied. Phong *et al.* (2015) proposed a novel method for estimating external forces acting on a 4-DOF robot manipulator's end effector using information from joint torque sensors (JTS). The algorithm combined time delay estimation (TDE) and input estimation technique with external forces as unknown input to the end effector to perform estimation. A modeling, parameter estimation and control of a robot with two degrees of freedom has been developed (Richter *et al.*, 2015). Their system is composed of a prosthetic leg with vertical displacement and hip angle attached to the robot and force plates were used for external force estimation. SonoMenegaldo (2009) presented a myoelectric hand prosthesis force control

through servo motor current feedback. DC motor actuator current was measured for real-time estimation of prehension (external) forces. This approach provided more accurate force estimation compared to open loop control, but the real-time estimation depended on the accuracy of the DC motor current which is prone to fluctuation.

Conventionally, heavy load cells are being employed to capture the ground reaction forces (GRFs) and moments in robotic and prosthesis leg during gait (Gonzalez, 2014). Using impedance controls, these data are used as feedbacks to control prosthetic legs of patients. However, the mammoth disadvantages of using load cells ranging from cost, integration difficulties, overload possibilities to high consumption of electric power has led many researchers to consider other ways of measuring parameters in prosthesis (Azimi *et al.*, 2018). Angle sensors are much more reliable, inexpensive and have accurate high resolution encoders (Fakoorian *et al.*, 2017). Hence, researchers are now considering angle sensors and other ways of estimating the system parameters from measurements of the output (Azimi *et al.*, 2018; Hamza *et al.*, 2020).

Generally, the Kalman filter (KF) and the extended Kalman filter (EKF) are frequently applied to these (nonlinear) systems to estimate the systems' state vectors from output measurements. Atkeson (2012) presented a technique that evaluated two approaches of developing Kalman filter for gait systems. The first model was referred to as LIPM KF (Linear Inverted-pendulum model Kalman filter) model and the second was planer Kalman filter model. Results obtained showed that the later slightly outperformed the former, although both were not optimal. The EKF is based on the linearization of the dynamics of the prosthesis systems utilizing Taylor series expansion. It is a good estimator and performed satisfactorily well in the speed estimator of an induction motor drive (Shi *et al.*, 2002), and to estimate values descriptive of the pack's present operating conditions in battery management systems (Plett, 2004). Therefore, a continuous time Extended Kalman Filter (EKF) has been proposed to estimate both the state vectors and ground reaction forces (GRFs) acting on a prosthetic foot (Fakoorian *et al.*, 2016). Though EKF estimation method performs well in some systems, it is prone to cumulative errors due to the gradient-based linearization it performs (Rigatos, 2011). It is also difficult to implement and only reliable for systems which are almost linear on the time scale of the update intervals (Julier and Uhlmann, 1997).

To mitigate the errors of the EKF method, Fakoorian *et al.* (2017) used unscented Kalman filter (UKF) to estimate the states and ground reaction forces acting on a prosthetic leg. The UKF outperformed EKF because it does not require the computation of Jacobian matrices and it is not based on local linearization of nonlinear dynamics. But the UKF updates sigma points at each iteration, as such it has a high computational cost. To overcome the drawbacks inherent in the aforementioned methods, Rigatos (2011) had introduced a derivative-free Kalman filtering (DKF) suitable for state estimation-based control of a class of nonlinear systems and capable of estimating the state vectors of the nonlinear system without on-line derivative and Jacobian calculations. Moosavi

*et al.* (2017) used a derivative-free Kalman filter (DKF) for state estimation-based control for a n-DOF prosthetic system along with PD and PI disturbance compensators, as supervisory control terms for the rejection of disturbances. Due to the profound negative effect of Kalman filter's process - noise covariance matrix (Q) and measurement noise covariance matrix (R) - on the filter's performance, some authors have proposed an intelligent way of determining these covariance matrices using optimization techniques. Such as: a Genetic Algorithm optimized extended Kalman filter (EKF) for speed estimation of an induction motor drive (Shi *et al.*, 2002), and a fruit fly optimized Kalman filter algorithm for pushing distance estimation of a hydraulic powered roof support through tuning covariances (Zhang *et al.*, 2016). The potentials of bio-inspired optimization algorithms are yet to be fully utilized in human prosthetic systems.

Hence, to further improve the accuracy of the artificial prosthetic systems, we propose an optimized derivative-free Kalman filter (DKF) for the estimation of external forces and states of transfemoral amputees while reducing material costs. The system has four degrees of freedom (vertical displacement, thigh angle, knee angle and ankle angle). The plant, being nonlinear, is transformed to its linear equivalent using differential flatness. Optimization algorithms have been used in order to improve the performance of artificial prosthetic systems; the optimization method deployed is known as Grasshopper Optimization algorithm developed by Saremi *et al.* (2017). Elsewhere, Ron Davis (2014) proposed an evolutionary optimization of ground reaction for a prosthetic leg testing robot using bio-inspired optimization algorithm called biogeography-based optimization (BBO) to optimize the hip motions of the robot. Grasshopper optimization was employed in this work to optimize the parameters of the derivative-free Kalman filter by minimizing the root mean square estimation error of the nonlinear filter. In our method, the process noise covariance matrix (Q) and measurement covariance matrix (R) which used to be obtained using trial and error approach was tuned using Grasshopper optimization algorithm, this minimizes the computational root mean square error. This is the main contribution of this paper. This significantly reduced the root mean square error (RMSE) of the Derivative free Kalman Filter making it optimal. The optimized value of Q and R were used in the application of the standard Kalman filtering methodology to estimate not just the states (joint angle displacements and velocities) but also the GRF's acting on the system. The rest of the paper is organized as follows: Section 2 presents the system model and its linearization using differential flatness followed by the application of the Grasshopper Optimization to optimize the parameters of the derivative-free Kalman filtering is in Section 3. The application of the standard Kalman filtering methodology using the optimal values obtained through Grasshopper Optimization comes in Section 4. In Section 5, the simulation and results of the designed filter are presented while Section 6 concludes the study.

## 2. System model and linearization

The prosthesis system for transfemoral amputees considered has four degrees of freedom (vertical displacement, thigh angle, knee angle and ankle angle). Since Kalman filtering applies directly to linear systems, the plant model (which is nonlinear) is transformed to its linear equivalent using differential flatness. Applying the standard Kalman filter to a nonlinear system through the transformation of the nonlinear system to the observer canonical form is called derivative-free Kalman filtering (DKF). The model of the prosthetic leg is based on the standard robotic Newtonian framework. The general dynamic model of the system is given as follows (Fakoorian *et al.*, 2016):

$$D(q)\ddot{q} + C(q, \dot{q})\dot{q} + B(q, \dot{q}) + J_e^T F_e + G(q) = u \quad (1)$$

Where  $q^T = [q_1, q_2, q_3, q_4]$  is the vector of joint displacements,  $q_1$  is vertical hip displacement,  $q_2$  is thigh angle,  $q_3$  is knee angle, and  $q_4$  is ankle angle,  $D(q)$  is the inertia matrix,  $C(q, \dot{q})$  is a matrix accounting for centripetal and Coriolis effects,  $B(q, \dot{q})$  is a nonlinear damping vector,  $J_e$  is the kinematic Jacobian relative to the point of application of the external forces  $F_e$ ,  $G(q)$  is the gravity vector, and  $u$  is the four-element vector of control signals. Equation (1) is obtained using Euler-Lagrange method. A treadmill is used to simulate the walking surface of the system. The ground reaction force (GRF) model is given as follows (Fakoorian *et al.*, 2016).

$$z_h = -a_H \sin\left(q_2 + q_3 + q_4 + \left(\frac{\pi}{2} + \cos^{-1}\left(\frac{a_h}{a_H}\right)\right)\right) + l_3 \sin(q_2 + q_3) + l_2 \sin(q_2) + q_1 \quad (2)$$

$$z_t = -a_T \sin\left(q_2 + q_3 + q_4 + \left(\frac{\pi}{2} + \cos^{-1}\left(\frac{a_h}{a_T}\right)\right)\right) + l_3 \sin(q_2 + q_3) + l_2 \sin(q_2) + q_1 \quad (3)$$

$$F_{zh} = -k_b(z_h - s_z) \left(\frac{1 + \text{sign}(s_h - s_z)}{2}\right) \quad (4)$$

$$F_{zt} = -k_b(z_t - s_z) \left(\frac{1 + \text{sign}(s_t - s_z)}{2}\right) \quad (5)$$

$$F_{xh} = \beta F_{zh} \quad (6)$$

$$F_{xt} = \beta F_{zt} \quad (7)$$

Where  $k_b$  is the stiffness of the belt,  $l_2$  and  $l_3$  are the lengths of the thigh (link 2) and shank (link 3) respectively,  $s_z$  is treadmill standoff,  $a_h$  is the height of the ankle joint above the sole of the foot,  $a_H$  is the distance from the ankle joint to the heel and  $a_T$  is the distance from the ankle joint to the toe,  $\beta$  is the coefficient of friction between the foot and the belt.  $z_t$  and  $z_h$  which are the vertical positions of the toe and heel are shown in Figure 1.

During our simulation we assumed that the prosthetic leg walks along x-axis. A foot with two points ground contact was used as shown in Figure 1, after toe-off there is no foot contact to the ground which implies the ground reaction force (GRF) is equal to zero. Assuming that after toe-off the external force  $F_e = 0$ , (1) can be transformed to its flat output as (Fakoorian *et al.*, 2016):

$$y = [q_1, q_2, q_3, q_4] = [x_1, x_3, x_5, x_7] \quad (8)$$

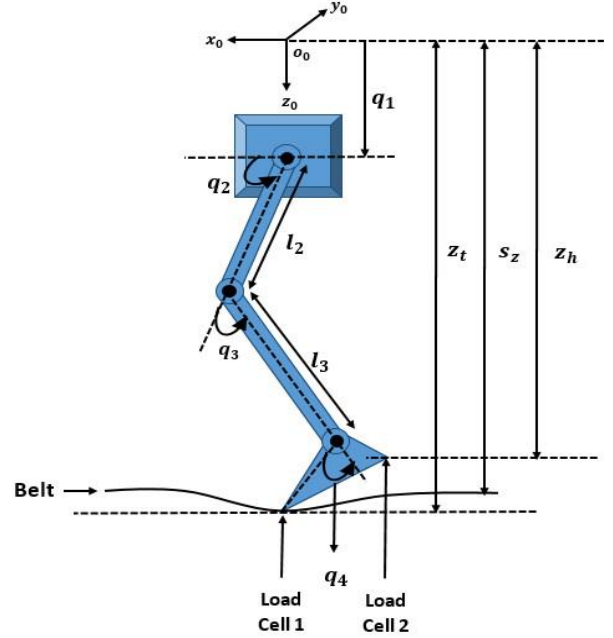


Figure 1: Prosthetic leg model (Fakoorian *et al.*, 2016).

All the system variables can be written as a function of flat output  $y$  and its successive derivatives. From the work of Fakoorian *et al.* (2016), the control input  $u$ , can also be written as a function of  $y$  and its successive derivatives as given in (9).

$$u = \begin{pmatrix} G_1 h(y, \dot{y}) \\ G_2 h(y, \dot{y}) \\ G_3 h(y, \dot{y}) \\ G_4 h(y, \dot{y}) \end{pmatrix}^{-1} \left\{ \begin{matrix} [1000] \ddot{y}^T \\ [0100] \ddot{y}^T \\ [0010] \ddot{y}^T \\ [0001] \ddot{y}^T \end{matrix} \right\} - \begin{pmatrix} f_1 h(y, \dot{y}) \\ f_2 h(y, \dot{y}) \\ f_2 h(y, \dot{y}) \\ f_3 h(y, \dot{y}) \end{pmatrix} \quad (9)$$

Considering the state vector  $x \in R^{8 \times 1}$ , with the state variables, the following matrices are defined.

$$A = \begin{pmatrix} 0 & 1 & 0 & 0 & 0 & 0 & 0 & 0 \\ 0 & 0 & 0 & 0 & 0 & 0 & 0 & 0 \\ 0 & 0 & 0 & 1 & 0 & 0 & 0 & 0 \\ 0 & 0 & 0 & 0 & 0 & 0 & 0 & 0 \\ 0 & 0 & 0 & 0 & 0 & 1 & 0 & 0 \\ 0 & 0 & 0 & 0 & 0 & 0 & 0 & 0 \\ 0 & 0 & 0 & 0 & 0 & 0 & 0 & 1 \\ 0 & 0 & 0 & 0 & 0 & 0 & 0 & 0 \end{pmatrix} \quad C = \begin{pmatrix} 1 & 0 & 0 & 0 & 0 & 0 & 0 & 0 \\ 0 & 0 & 1 & 0 & 0 & 0 & 0 & 0 \\ 0 & 0 & 0 & 0 & 1 & 0 & 0 & 0 \\ 0 & 0 & 0 & 0 & 0 & 0 & 1 & 0 \\ 0 & 0 & 0 & 0 & 0 & 0 & 0 & 1 \end{pmatrix}$$

Therefore, the system satisfies the differential flatness properties and can be transformed into linear canonical form given by

$$\dot{x} = Ax + Bv \quad (10)$$

$$y = cx$$

Where the new input  $v$  is given by;

$$v = \begin{pmatrix} f_1(x, t) \\ f_2(x, t) \\ f_3(x, t) \\ f_4(x, t) \end{pmatrix} + \begin{pmatrix} G_1(x, t) \\ G_2(x, t) \\ G_4(x, t) \\ G_4(x, t) \end{pmatrix} u + \begin{pmatrix} \tilde{d}_1 \\ \tilde{d}_2 \\ \tilde{d}_2 \\ \tilde{d}_3 \end{pmatrix} \quad (11)$$

The DKF can be used for estimation-based control of robots if the robot model is subjected to a linearization transformation for exact feedback linearization control and then state estimation is performed on the linearized model with a standard Kalman filter.

### 3. Optimization of the derivative-free Kalman filter Parameters

Since it is necessary to choose the process noise covariance Q and measurement noise covariance R in a way that our model will converge quickly, choosing wrong Q and R can lead to large estimation error or the system diverging. There are multiple ways of doing this. The simplest method will be to guess and test until we get a satisfactory result i.e., using trial and error. A better method will be to optimize the Q and R values. This is what has been chosen in this research. The grasshopper optimization algorithm is used to optimize the values of the process and measurement noise covariance matrices by minimizing the RMSE of the Derivative Kalman filter thereby making it optimal. The equation to explore and exploit the search space in Grasshopper optimization is given as (Mirjalili et al., 2017):

$$X_i = c \left( \sum_{j=1, j \neq i}^N c \frac{(ubd-lbd)}{2} \times \frac{s(|X_j - X_i|)(X_j - X_i)}{d_{ij}} \right) + \times \hat{T}_d \quad (12)$$

Where;

$$c = c_{max} - l \times \frac{c_{max} - c_{min}}{L}$$

$$s(r) = f e^{-\frac{r}{L}} - e^{-r}$$

$c_{max}$  is the maximum value,  $c_{min}$  is the minimum value,  $l$  indicates the current iteration, and  $L$  is the maximum number of iterations, 1 and 0.00001 is used for  $c_{max}$  and  $c_{min}$  respectively.  $f$  indicates the intensity of attraction and  $L$  is the attractive length scale.  $ubd$  is the upper bound in the  $D^{th}$  dimension,  $lbd$  is the lower bound in the  $D^{th}$  dimension,  $\hat{T}_d$  is the value of the  $D^{th}$  dimension in the target (best solution found so far). The cost function is given by:

$$Cost = RMSE_{min} = \left[ \frac{1}{n} \sum (x - \tilde{x})^2 \right]^{1/2} \quad (13)$$

Where  $x$ ,  $\tilde{x}$  and  $n$  are actual state, estimated state and the number of states respectively.

Initial values chosen for Q and R, are:

$$Q = ([0.0005, 0.0005, 0.0005, 0.0005, 0.0002, 0.0002, 0.0002, 0.0002])$$

$$R = \text{diag}([10^{-3}, 10^{-3}, 10^{-3}, 10^{-3}])$$

The lower bound for Q and R is given by

$$Q = \text{diag}([0.0000, 0.0000, 0.0000, 0.0000, 0.0000, 0.0000, 0.0000, 0.0000])$$

$$R = \text{diag}([10^{-5}, 10^{-5}, 10^{-5}, 10^{-5}])$$

The upper bound for Q and R will be

$$Q = \text{diag}([100, 100, 100, 100, 100, 100, 100, 100])$$

$$R = \text{diag}([10^{-1}, 10^{-1}, 10^{-1}, 10^{-1}])$$

The process of calculating the fitness will be running the Derivative-free Kalman filter algorithm. After the DKF is run for all the search agents, the one that yields the least RMSE will be chosen as the optimal value.

### 4. Application of Standard Kalman filtering methodology using the optimal values of DKF

The Kalman filter is applied directly to linear systems. However, to implement a derivative free Kalman filter, a nonlinear system dynamic can be transformed into canonical form using differential flatness theory and a standard Kalman filtering is applied to the transformed model.

The initial state  $x(0)$  is a random vector with covariance  $p(0)$

$$x(0) = E[x(0)]$$

$$P(0) = E[(x(0) - \hat{x}(0))(x(0) - \hat{x}(0))^T]$$

The DFK equations are as follows

$$\dot{x} = f(\hat{x}, u, t) + K[y - h(\hat{x}, t)] \quad (14)$$

$$K(t) = P(t)C^T(t)R^{-1}(t) \quad (15)$$

$$\begin{aligned} \dot{P} = & A(t)P(t) + P(t)A(t) + Q(t) \\ & - P(t)C^T(t)R^{-1}(t)C(t)P(t) \end{aligned} \quad (16)$$

State estimation of the system variables was performed using a nonlinear observer (estimator), Equations (8) and (9), then the estimated states of the system could be substituted into the GRF model Equation (2) to Equation (7) to obtain GRF estimates. This approach was used in this research because it is more flexible compared to other approaches. Four measurement sensors were used (vertical displacement, thigh angle, knee angle and ankle angle) and the performance of the prosthesis system in normal gait mode was examined. The design of an Optimized Derivative-Free Kalman Filter for estimation of external forces acting on a lower limb prosthetic leg and states of the system was simulated using MATLAB 2018Ra simulation environment. The complete simulation set up for the prosthesis system is shown in Figure 2.

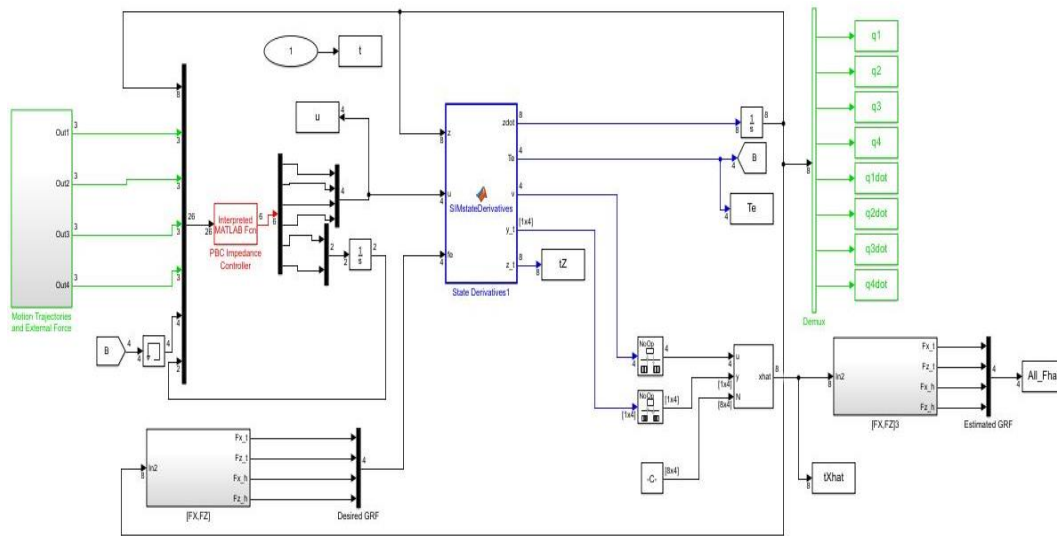


Figure 2: Complete Simulink block model

### 5. Simulation and Results

In the prosthetic leg, we have 8 states, so the A matrix is 8x8 as presented in Equation (10). Four states were used as measurements: vertical hip displacement, thigh angle, knee angle and ankle angle, this implies that the dimension of the C matrix is 4x8 as presented in Equation (11). Previous authors used load cells or sensors directly fixed on the system to obtain the external forces (Veltink *et al.*, 2005; Aubin *et al.*, 2011). The use of force sensors to obtain the external forces does not only make the system heavy and complex, but also relatively costly.

The performance of the optimized derivative-free nonlinear Kalman Filter was tested in the nonlinear state estimation-based control for a 4-DOF rigid-link prosthetic leg given in Figure 1. The flat outputs were taken to be the prosthetic leg’s joint angles  $y_1 = x_1, y_2 = x_3, y_3 = x_5$  and  $y_4 = x_7$ . It has been proven that all state variables of the prosthetic model and the associated control inputs can be written as functions of the flat output  $[y_1, y_2, y_3, y_4]$  and of the associated derivatives. The position and velocity variations for the first joint of the prosthetic leg are depicted in Figure 3. For the second joint of the prosthetic leg the tracking of the position and velocity reference is depicted in Figure 4, Figure 5 shows the position and velocity of the third joint and Figure 6 shows the position and velocity of the fourth joint.

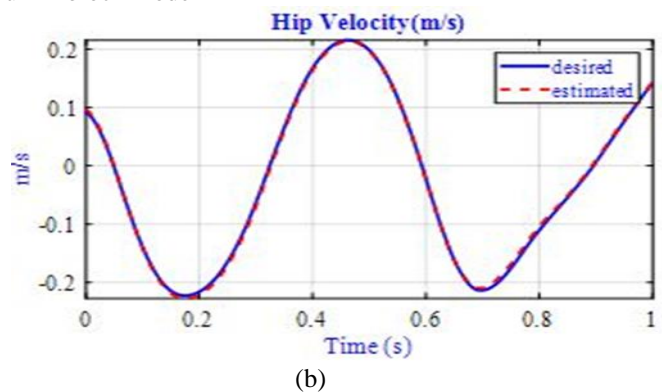
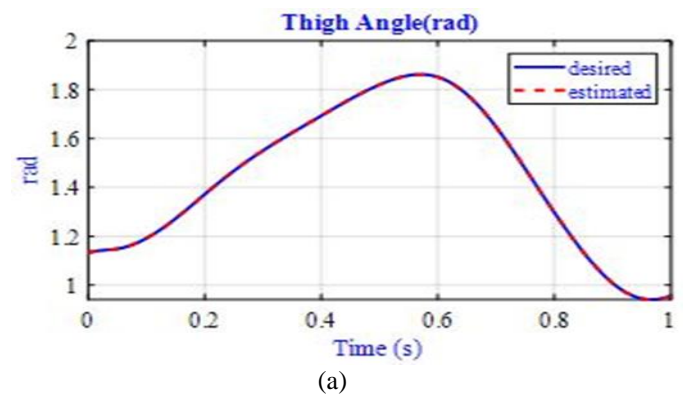
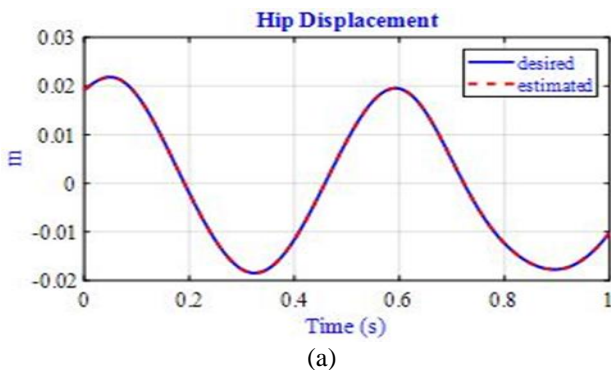
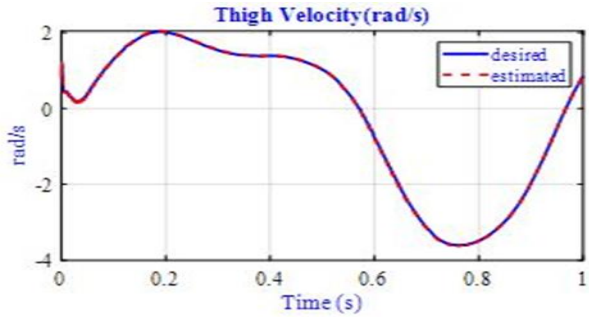


Figure 3: a) hip displacement b) hip velocity

In this Optimized-DFK simulation result shown in Figure 3, **a** is the tracking of a reference data position (blue line) by the angle ( $q_1$ ) of the first joint of the prosthetic leg (red dotted line) while **b** is the tracking reference data velocity (blue line) by the angular velocity ( $\dot{q}_1$ ) of the first joint of the prosthetic leg (red dotted line).

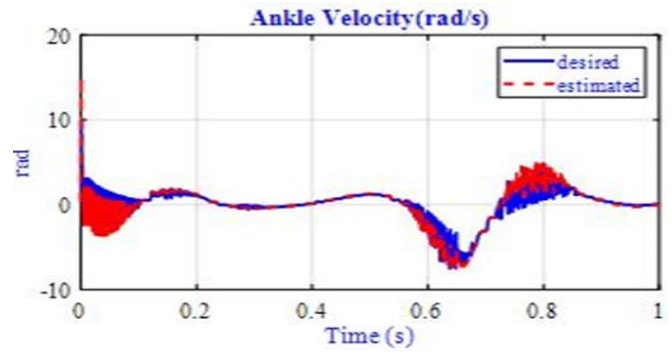
From Figure 4, **a** is the tracking of a reference data position (blue line) by the angle ( $q_2$ ) of the second joint of the prosthetic leg (red dotted line) and **b** is the tracking reference data velocity (blue line) by the angular velocity ( $\dot{q}_2$ ) of the second joint of the prosthetic leg (red dotted line).





(b)

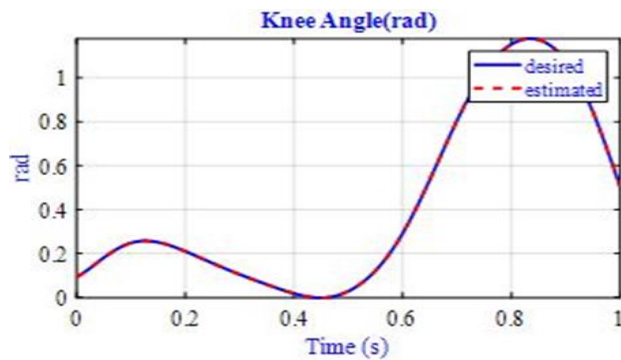
Figure 4: a) Thigh angle b) Angular velocity of the thigh



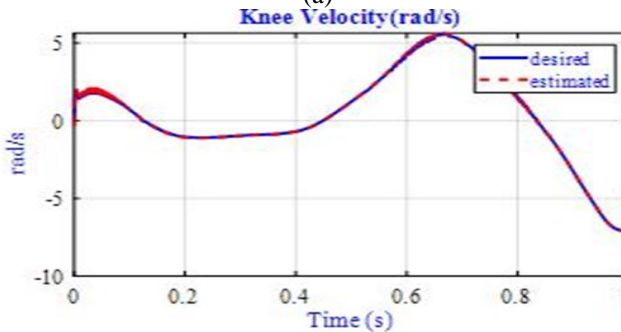
(b)

Figure 6: a) Ankle angle b) Angular velocity of the ankle

Figure 6 (a) shows tracking of a reference data position (blue line) by the angle ( $q_4$ ) of the fourth joint of the prosthetic leg (red dotted line), while Figure 5 (b) shows tracking reference data velocity (blue line) by the angular velocity ( $\dot{q}_4$ ) of the fourth joint of the prosthetic leg (red dotted line). The results presented in the figures above show that the optimized-DFK converge to true states and was able to accurately estimate the displacements and velocities of the joint angles of the system.



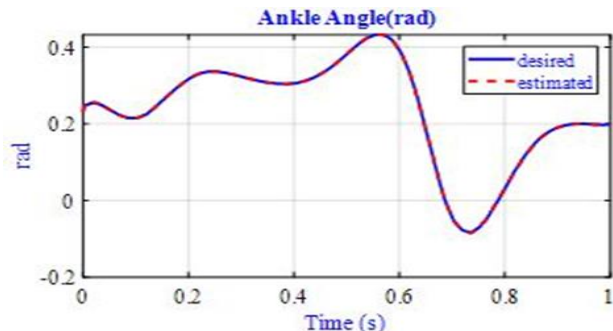
(a)



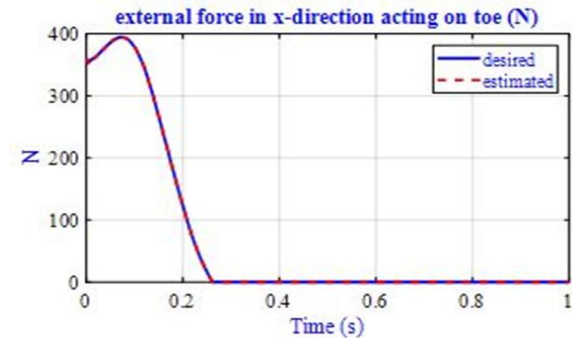
(b)

Figure 5: a) Knee angle b) Angular velocity of the knee

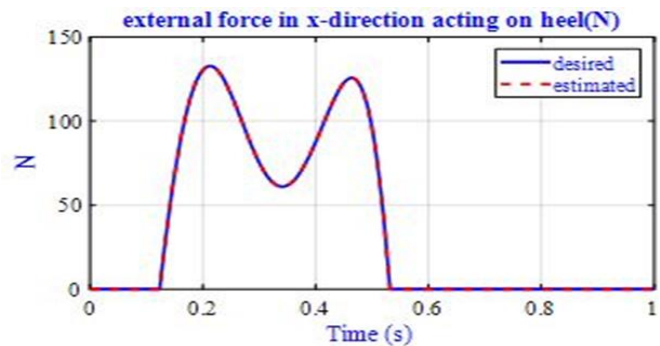
In Figure 5, **a** depicts the tracking of a reference data position of the Optimized-DFK (blue line) by the angle ( $q_3$ ) of the third joint of the prosthetic leg (red dotted line). **b** tracking reference data velocity (blue line) by the angular velocity ( $\dot{q}_3$ ) of the third joint of the prosthetic leg (red dotted line).



(a)



(a)



(b)

Figure 7: Vertical ground reaction force

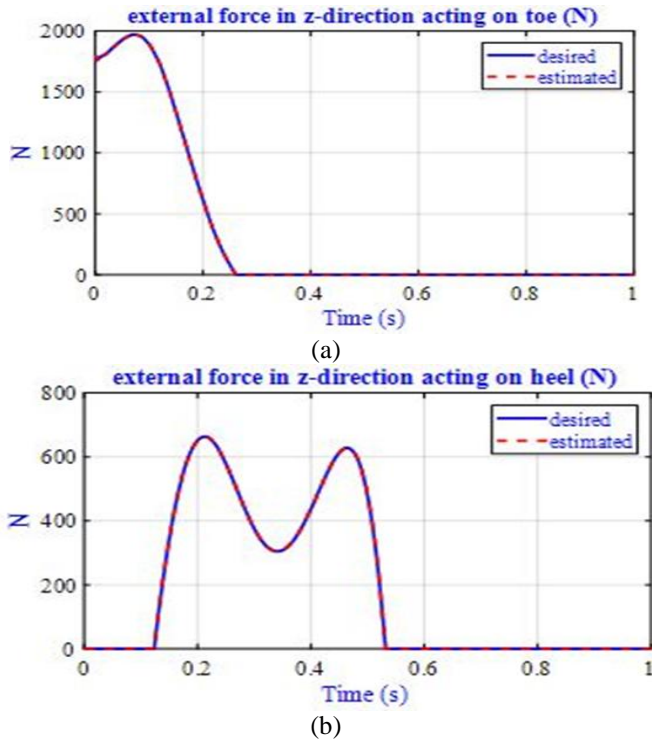


Figure 8: Horizontal ground reaction force

The ground reaction force estimation results are shown in figure 7 and 8. After toe-off the ground reaction force is zero (GRF=0) because there is no contact between the foot and the ground. After substituting the estimated state value into the GRF model, it can be observed that the optimized-DFK converges and accurately estimated the actual GRFs values.

Table 1: Comparison of average RMSE between EKF, UKF and Optimized-DKF

Nonlinear Filter	Ave. RMSE of Positions	Ave. RMSE of Velocities	Ave. RMSE of GRFs
EKF	0.0020	0.1205	11.8525
UKF	0.0016	0.0896	7.9792
Optimized-DKF	0.000005	0.2379	0.0222
Average % Improvement	99.85		99.77

The average RMSE of the Optimized-DKF is computed and compared with that of EKF and UKF as reported in (Fakoorian *et al.*, 2017). The results are shown in Table 1, and it is seen that the optimized-DFK outperformed both the EKF and the UKF in estimating the positions and the GRFs significantly. However, there is no improvement in the average RMSE of velocities compared to both EKF and UKF owing to the noise introduced on the system as result of the rotation of foot about the angle. Figure 8 depicts the zoomed region of angular velocity of the ankle, it can be seen that the optimized-DFK was able to estimate the stable part of the signal and has difficulty in estimating the noisy part of the signal. This is because of the rotation of foot about the ankle joint when the foot of the prosthetic leg hit the ground. Figure 6 shows the ankle angle ( $q_4$ ) estimate, when the ankle angle changes, the

foot rotates around the ankle which makes ankle angular velocity ( $\dot{q}_4$ ) noisy as depicted in Figure 9. This makes the estimator (optimized-DFK) relatively hard to track the angular velocity of the ankle owing to the difficult task in the compromise between noise rejection and bandwidth (Fakoorian *et al.*, 2017).

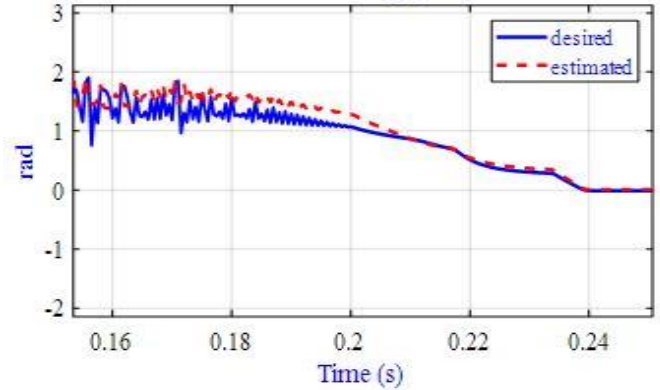


Figure 9: Zoomed region of the ankle velocity

## 6. Conclusion

This paper approached the problem of capturing external forces acting on the foot of a prosthetic leg. External force estimation is a better alternative than direct external force measurement because load cells have disadvantages of high cost, integration difficulty due to bulkiness and their proneness to errors. The differentially flat model of the prosthesis and its transformation to the canonical form has been analyzed. An optimized-DFK is developed in this work to estimate the states and the GRF's. Differential control theory is applied to obtain a linear equivalence of the system, a recently developed optimization algorithm known as GOA is used to optimize the parameters of DFK, and these optimized parameters together with the standard Kalman filter algorithm were applied to the resulting system to estimate not just the states (joint angle displacements and velocities) but also the GRF's acting on the system. The average root mean square estimation error (RMSE) of Extended Kalman Filter (EKF) for joint angles is 0.002 rad and 11.85N for ground reaction forces (GRFs), the corresponding values for Unscented Kalman Filter (UKF) is 0.0016rad and 7.9N while the values for the optimized-DFK are 0.000005rad for joint angle and 0.0222N for GRFs. This represents an average RMSE improvement of 99.85% and 99.77% estimation in joint angles and GRFs, when compared to EKF and UKF respectively.

## References

- Atkeson, C. G. (2012). *State estimation of a walking humanoid robot*. Paper presented at the Intelligent Robots and Systems (IROS), 2012 IEEE/RSJ International Conference on Intelligent Robots and Systems.
- Aubin, P. M., Whittaker, E., & Ledoux, W. R. (2011). A robotic cadaveric gait simulator with fuzzy logic vertical ground reaction force control. *IEEE transactions on robotics*, 28(1), 246-255.

- Awad, M., Abouhossein, A., Dehghani-Sanij, A., Richardson, R., Moser, D., Zahedi, S., & Bradley, D. (2016). Towards a smart semi-active prosthetic leg: preliminary assessment and testing. *IFAC-PapersOnLine*, 49(21), 170-176.
- Azimi, V., Nguyen, T. T., Sharifi, M., Fakoorian, S. A., & Simon, D. (2018). Robust ground reaction force estimation and control of lower-limb prostheses: Theory and simulation. *IEEE Transactions on Systems, Man, Cybernetics: Systems*, 50(8), 3024-3035.
- Behera, M., & Indalkar, A. G. (2020). Effectiveness of Suspension System in Transfemoral Prosthesis. *International Journal of Health Sciences and Research*, 10(9), 310-318.
- Fakoorian, S., Azimi, V., Moosavi, M., Richter, H., & Simon, D. (2017). Ground reaction force estimation in prosthetic legs with nonlinear Kalman filtering methods. *Journal of Dynamic Systems, Measurement, Control*, 139(11), 111004.
- Fakoorian, S. A., Simon, D., Richter, H., & Azimi, V. (2016). *Ground reaction force estimation in prosthetic legs with an extended Kalman filter*. Paper presented at the 2016 Annual IEEE Systems Conference (SysCon).
- Geng, Y., Xu, X., Chen, L., & Yang, P. (2010). *Design and analysis of active transfemoral prosthesis*. Paper presented at the IECON 2010-36th Annual Conference on IEEE Industrial Electronics Society.
- Geng, Y., Yang, P., Xu, X., & Chen, L. (2012). *Design and simulation of active transfemoral prosthesis*. Paper presented at the 2012 24th Chinese Control and Decision Conference (CCDC).
- Gonzalez, M. (2014). *Biomechanical Analysis of Gait Kinetics Resulting From Use of a Vacuum Socket on a Transtibial Prosthesis*. (Master Thesis), University of Nevada, Las Vegas, VD.
- Hamza, M. F., Ghazilla, R. A. R., Muhammad, B. B., & Yap, H. J. (2020). Balance and stability issues in lower extremity exoskeletons: A systematic review. *Biocybernetics and Biomedical Engineering Online*, 40(4), 1666-1679.
- Julier, S. J., & Uhlmann, J. K. (1997). *New extension of the Kalman filter to nonlinear systems*. Paper presented at the Signal processing, sensor fusion, and target recognition VI.
- Mirjalili, S., Saremi, S., & Lewis, A. (2017). Grasshopper optimisation algorithm: theory and application. *Advances in Engineering Software*, 105, 30-47.
- Moosavi, S. M., Fakoorian, S. A., Azimi, V., Richter, H., & Simon, D. (2017). *Derivative-free Kalman filtering-based control of prosthetic legs*. Paper presented at the 2017 American Control Conference (ACC).
- Phong, L. D., Choi, J., Lee, W., & Kang, S. (2015). A Novel Method for Estimating External Force: Simulation Study with a 4-DOF Robot Manipulator. *Journal of precision engineering and manufacturing*, 16, 755-756. doi:10.1007/s12541-015-0100-7
- Plett, G. L. (2004). Extended Kalman filtering for battery management systems of LiPB-based HEV battery packs: Part 1. Background. *Journal of Power sources*, 134(2), 252-261.
- Richter, H., Simon, D., Smith, W. A., & Samorezov, S. (2015). Dynamic modeling, parameter estimation and control of a leg prosthesis test robot. *Applied Mathematical Modelling*, 39(2), 559-573.
- Rigatos, G. G. (2011). A derivative-free Kalman filtering approach to state estimation-based control of nonlinear systems. *IEEE Transactions on Industrial Electronics*, 59(10), 3987-3997.
- Ron Davis, H. R., Dan Simon, Antonie van den Bogert. (2014). *Evolutionary Optimization of Ground Reaction Force for a Prosthetic Leg Testing Robot*. Paper presented at the American Control Conference (ACC), Portland, Oregon, USA.
- Saremi, S., Mirjalili, S., & Lewis, A. (2017). Grasshopper optimisation algorithm: theory and application. *Advances in Engineering Software*, 105, 30-47.
- Shi, K., Chan, T., Wong, Y., & Ho, S. L. (2002). Speed estimation of an induction motor drive using an optimized extended Kalman filter. *IEEE Transactions on Industrial Electronics*, 49(1), 124-133.
- Sono, T. S. P., & Menegaldo, L. L. (2009). Myoelectric hand prosthesis force control through servo motor current feedback. *Artificial Organs*, 33(10), 871-876.
- Varol, H. A., & Goldfarb, M. (2007). *Decomposition-based control for a powered knee and ankle transfemoral prosthesis*. Paper presented at the 2007 IEEE 10th International Conference on Rehabilitation Robotics.
- Veltink, P. H., Liedtke, C., Droog, E., & van der Kooij, H. (2005). Ambulatory measurement of ground reaction forces. *IEEE Transactions on Neural Systems Rehabilitation Engineering*, 13(3), 423-427.
- Windrich, M., Grimmer, M., Christ, O., Rinderknecht, S., & Beckerle, P. (2016). Active lower limb prosthetics: a systematic review of design issues and solutions. *Biomedical Engineering Online*, 15(3), 5-19.
- Zhang, L., Wang, Z., Tan, C., Si, L., Liu, X., & Feng, S. (2016). A fruit fly-optimized Kalman filter algorithm for pushing distance estimation of a hydraulic powered roof support through tuning covariance. *Applied Sciences*, 6(10), 299.
- Zhang, Z., Yu, H., Cao, W., Wang, X., Meng, Q., & Chen, C. (2021). Design of a Semi-Active Prosthetic Knee for Transfemoral Amputees: Gait Symmetry Research by Simulation. *Applied Sciences*, 11(12), 5328.